

Structure-Property Correlation in TRIP Aided Steels

Shiv Brat Singh^{1,*}, Tanmay Bhattacharyya^{1,2}, Ravi Ranjan¹, Sandip Bhattacharyya²,
Debashish Bhattacharjee²

¹Department of Metallurgical and Materials Engineering, IIT Kharagpur
²R&D and SS, Tata Steel Limited

Abstract The need for light-weight auto bodies with improved crash resistance and other safety parameters has encouraged the development of a new family of multi-phase steels having higher strength and better formability. High strength TRIP aided steel is the ideal material for such applications, but developing a grade that has good formability, coatability and weldability is a major challenge. The present work has been undertaken to address the issues of coatability and weldability as well as to target a high strength - ductility balance. The work includes Thermo Calc calculations to study the phase relationships, thermo-mechanical simulation, prediction of microstructure through artificial neural network and laboratory experiments in hot-dip galvanising simulator. Routine characterisation was done for the assessment of microstructure and properties. Three experimental steels were prepared in a vacuum induction furnace. The as-cast ingots were forged and then hot and cold rolled. Laboratory salt bath heat treatment of the cold rolled samples was carried out following the standard two-step heat treatment cycle consisting of intercritical annealing and isothermal bainitic transformation to obtain the desired microstructure and target mechanical properties. As a part of weldability assessment, the heat treated samples were spot welded. A difficulty with TRIP steels is their poor wettability during galvanising due to the formation of oxides of silicon on the surface. Two of these three test grades had aluminium as the replacement for silicon to improve wettability. Dew point during thermal processing plays a critical role and affects the wettability. The two-step heat treatment described above followed by hot dip galvanising was simulated with varying dew points in hot dip galvanising (Rhesca) simulator to assess the coatability of the samples. Very good strength-elongation balance was obtained for all the three steels and the samples with lower silicon and higher dew point showed better wettability and coatability. Weldability studies revealed that the introduction of post weld tempering cycles improves the weld nugget geometry, breaking load and failure mode under tensile shear loading. Tensile studies at high strain rate revealed a satisfactory performance of the steel even at 100 s⁻¹ suggesting the fitness to be used at the crash prone zones of automobiles.

Keywords TRIP (Transformation Induced Plasticity), Wettability, Weldability, Crash Resistance Crumpling

1. Introduction

The need for addressing stringent environment and safety norms has compelled the automakers to design light-weight auto bodies with enhanced crash resistance. A new family of multi-phase steels having higher strength and better formability, named Transformation induced plasticity (TRIP) aided steel is gaining popularity to satisfy the demand as it has been adjudged as the most promising solution for the production of cars with low body mass because of the combination of high strength and large uniform elongation that they offer. The TRIP effect arises from deformation induced transformation of retained austenite to martensite[1]. It is accompanied by an invariant plane strain shape deformation as well as a volume expansion. This results in a higher strain hardening rate that delays the onset of necking,

eventually resulting into higher uniform and total elongation [2]. An important feature of steels of this genre is enhanced ductility at a very high strength level[3]. TRIP effect enhances the mechanical properties by two mechanisms[4, 5]: (i) composite strengthening via the formation of hard martensite particles dispersed in the ferrite matrix and (ii) formation of dislocations around newly formed martensite regions as a result of the volumetric expansion during the austenite to martensite transformation.

This steel is ideal for passive safety structural applications like bumper reinforcement, door impact beam etc., due to its high strain hardening rate and dynamic energy absorption capacity[6]. The microstructure of conventional TRIP aided steels comprises ferritic matrix (~55-65%) along with bainite (~25-35%) and metastable retained austenite (~5-20%)[7]. The TRIP effect depends on the amount of retained austenite and its stability to deformation induced transformation.

Conventionally, TRIP aided steels contain about 1.5 wt% silicon which enhances the volume fraction and stability of the retained austenite by suppressing cementite formation during the isothermal bainitic transformation[8]. The

* Corresponding author:

sbs22@metal.iitkgp.ernet.in (Shiv Brat Singh)

Published online at <http://journal.sapub.org/ijmee>

Copyright © 2013 Scientific & Academic Publishing. All Rights Reserved

solubility of Si in cementite is very small and therefore formation of a cementite nucleus in the presence of Si requires the diffusion controlled ejection of Si at the transformation front, causing a build up in the concentration of Si around the cementite nucleus. This locally increases the activity of carbon resulting in lowering of the flux of carbon and hence inhibits the development of cementite embryos[9]. Inhibition of carbide formation allows austenite to inherit a large amount of carbon, which lowers the M_s (martensite start) temperature and thus a considerable amount of metastable austenite is retained at room temperature[10].

Conventional TRIP aided steel with high silicon (1.5 wt%) suffers from poor wettability during galvanising due to deleterious effect of silicon. It is reported that silicon in concentration higher than 0.5 wt% is detrimental to coatability[11]. High Si leads to poor weldability as well[12]. To avoid these problems silicon can be partially replaced by aluminium[13, 14, 15]. Aluminum, like silicon, is insoluble in cementite and helps in retarding cementite formation. Al facilitates coatability by forming an inhibition layer on the steel surface, which in turn prevents the formation of Si/Mn oxides and bare spots. However, aluminum is a weak solid solution strengthening element; complete replacement of silicon by aluminum is not suggested as these Al-containing steels cannot reach the strength level possible with Si alloyed steel[1]. Moreover, Chen *et al.*[16] have shown that Si level should be more than 0.8 wt% to obtain reasonable amount of retained austenite. Of late, addition of microalloying elements for enhancing the strength level has become very popular[17]. Niobium is considered to be very effective amongst these, especially for the steels where silicon is replaced either partially or fully by aluminum[17]. The effect of Nb addition is rather complex. It helps refine austenite formed during the intercritical annealing[18] which can lead to formation of some pro-eutectoid ferrite during cooling to the isothermal bainite transformation temperature and consequent carbon enrichment of the untransformed austenite. The finer grain size increases the stability of austenite by reduction of M_s (martensite start) temperature [18]. Niobium in solid solution retards recrystallisation of austenite, and the kinetics of austenite to ferrite transformation[17]. It also inhibits recrystallisation by strain induced precipitation. Furthermore, it increases the relative amount of retained austenite by approximately 25%, which can significantly improve the mechanical properties of the steel[19, 20]. Niobium accelerates the bainite reaction, particularly at the temperature of galvannealing[21]. As a result of increased bainite formation at a faster rate, it is possible to enrich the remaining austenite with carbon and stabilize it. It is thus possible to retain austenite in the final microstructure, even at the relatively low times of holding during galvannealing in a continuous line[21]. Therefore, microalloying, especially with niobium, attracts research studies in the area of development of new generation TRIP aided steels.

P added TRIP-assisted steel[1] imparts solid solution strengthening and increases the stability of retained austenite.

Oxides of phosphorous segregates at α -Fe grain boundary resulting in reduction of boundary-flux and the extent of oxide formation on surface[22]. It also decreases the inter-diffusion of Fe and Zn, favours G1 formation and hinders Γ . It is more amenable to wetting by molten zinc. It is reported that P is not harmful from the point of view of embrittlement and as well as spot weldability up to 0.1 wt% for such steel compositions[23].

Apart from alloy engineering, process optimization is also considered to be an important means for improvement of coatability. It is reported that if the hot dipping is done after a combination of intercritical annealing and isothermal bainitic transformation in a furnace atmosphere with a high dew point, the wettability improves significantly for conventional 1.5 wt% Si TRIP-aided steel. However, still some bare spots are unavoidable for CMnSi TRIP steel. On the contrary, the Si free CMnAl TRIP steel has a much better wettability when annealed at a low dew point. Therefore, dew point plays a crucial role for the surface quality of the steel and the wetting phenomenon in zinc bath during hot dip galvanizing[24].

Integration of automotive structures made up of high strength/ advanced high strength steels are predominantly carried out through resistance spot welding (RSW) process due to consistency in quality as well as high productivity. But there is a large gap area to specify optimal welding conditions for TRIP-aided steels having relatively richer alloying additions, such as high Si, always deteriorate weldability[25, 26]. Better coatability during galvanizing of TRIP-aided steel necessitates major alloy engineering. It has invited renewed challenge for welding of TRIP-aided steel[27].

The weldability of 'low carbon low alloyed' TRIP-aided steel faces severe complexities. After solidification, welds become very hard and can show a brittle behavior. The hardness of the heat affected zone (HAZ) attains to the tune of 500 HV and more[28], and cold cracking phenomenon is very prone to occur. During resistance spot welding, especially, the interface between the plates can act like a notch and promotes fracture of the weld. It becomes very severe during coach peeling/ shear tensile fracture which usually produces partially interfacial fracture (inferior in terms of ductility) as opposed to full button peel off/ plug type (superior)[29].

The high strain rate properties of steel indicates the performance of the same under crash condition. It is already established that TRIP-aided steels are used in the crumpling zone of a car because of their high strain rate performance and ability of large dynamic energy absorption. Therefore, dynamic testing is of special interest for the steel grades under discussion. Yield stress and ultimate tensile strength of TRIP aided steel increase continuously as it occurs for ferritic steels, but showing a smaller slope. At very high strain rate the elongation values of these steels are as high as under quasistatic testing conditions or even higher. This behavior is probably correlated to adiabatic heating. The used test set up and specimen size can lead to a local

temperature increase up to 120 K. TRIP steel shows very good energy absorption quality even if at 200 s^{-1} strain rate [30]. Both temperature and strain rate affect the retained austenite transformation. At high strain rates, the uniform elongation decreases, whereas the total elongation and energy absorption increase. With raising test temperature, the tensile strength is reduced and the mechanical properties generally deteriorate, especially at $110 \text{ }^\circ\text{C}$. However,

excellent mechanical properties are obtained at $50 \text{ }^\circ\text{C}$ and $75 \text{ }^\circ\text{C}$ [31].

High strain rate properties being the indicator of performance under crash condition, a detailed study on tensile behaviour under dynamic loading has been presented for a simulated performance under crash condition with an overview on the study of wettability (coating performance during hot dip galvanising) and weldability.

2. Selection of Materials and Processing Parameters

Three steels were selected for this work. The compositions are shown in Table 1.

Table 1. Composition (wt%)

Grade	C	Mn	S	P	Si	Al	Nb
Grade 1 CMnSiAlP	0.22	1.43	0.007	0.065	0.62	1.18	0.003
Grade 2 CMnSiAlNb	0.21	1.58	0.008	0.017	0.66	1.30	0.032
Grade 3 CMnSiNb	0.20	1.36	0.015	0.015	1.69	0.009	0.035

As reported in previous works [32, 33] the details about transformation phenomena are collated in Table 2.

Table 2. Transformation temperatures, phase fraction calculation in the intercritical region and predicted values of retained austenite for the selected process parameters

Grade	Transformation Temperature ($^\circ\text{C}$)	
	Thermo-Calc	Gleeble
1: CMnSiAlP	Ae ₁ :731 Ae ₃ :1093	Ac ₁ :742 Ac ₃ :1125
2: CMnSiAlNb	Ae ₁ :735 Ae ₃ :1100	Ac ₁ :739 Ac ₃ :1135
3: CMnSiNb	Ae ₁ :709 Ae ₃ :867	Ac ₁ :746 Ac ₃ :985

Based on the philosophy elucidated in previous works [32- 34], the process parameters were set with the help of simulated information, Artificial neural network (ANN) work on prediction of microstructure, existing facilities for laboratory heat making, forging, hot rolling, cold rolling as well as two stage annealing followed by hot dip galvanizing in hot dip process simulator (Rhesca). The process flow including assessment plans is depicted in Fig. 1.

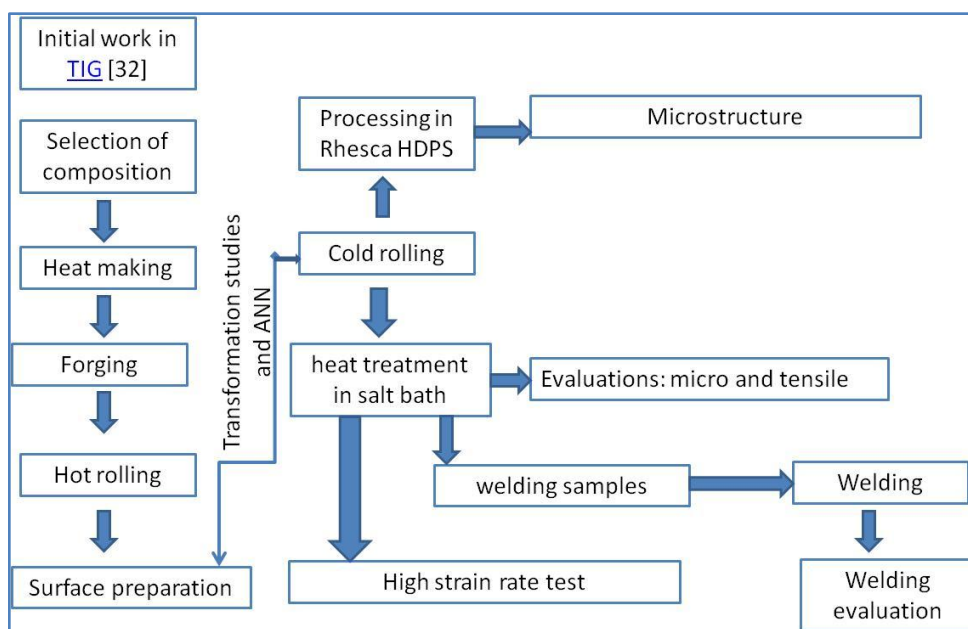


Figure 1. Process flow

Table 3. Results of mechanical test of the samples from HDPS (Rhesca) trial (average of three samples from every individual cycle, IBT: Isothermal bainitic transformation 450°C/120s, IA: Intercritical annealing: mentioned in the Table)

Grade	Yield strength (YS) (MPa)	Ultimate tensile strength (UTS) (MPa)	Uniform elongation (%)	Total elongation (%)	n- value	UTS x Total elongation (MPa %)
Grade 1 CMnSiAlP IA: 800°C/60s	485	795	31	36	0.34	28620
Grade 2 CMnSiAlNb IA: 800°C/60s	511	849	23	29	0.27	24621
Grade 3 CMnSiNb IA: 790°C/60s	521	959	19	23	0.26	22057

In the present work, samples were selected from the two stage heat treatment cycle as elaborated in the tables. For quasistatic tensile test, the samples were collected from HDPS (Hot Dip Process Simulator, Rhesca) trial

The quasistatic tensile test results revealed a good combination of strength and elongation and a logically good uniform elongation and n- value. The microstructural evaluation (Table 4) revealed presence of reasonable amount of retained austenite which could lead to have TRIP properties. For further work, under the purview of the paper, samples processed through the above cycles (grade specific) had been chosen.

Table 4. Comparison of the amount of experimentally measured retained austenite with that predicted using ANN

Sample	%RA in microstructure (based on optical vis-a-vis XRD examination)	%RA from ANN
Grade 1 CMnSiAlP For IA: 800°C/60s	9	12
Grade 2 CMnSiAlNb For IA: 800°C/60s	13	12
Grade 3 CMnSiNb For IA: 790°C/60s	8	6

(IBT for all cases 450°C/120s)

As reported previously[33], a very good match was observed between the retained austenite predicted through ANN and actually achieved experimentally[Table 4]. Also, The volume fraction of retained austenite measured through optical metallography had a reasonably good match with the value obtained through XRD technique[33].

3. Performance Appraisal of Wettability and Weldability Study

Wettability (coating performance during hot dip galvanizing in Rhesca HDPS):

An assessment[34] of the coating quality revealed that the

steels with silicon level lower than that of conventional (1.5% silicon) TRIP-aided steel showed better wettability, coating thickness and adherence property. At higher dew point (+ 5°C) during, the coatability was much improved than that at the lower dew point (- 40°C). The rationale for the same is as follows: for the steel grades where silicon is partially replaced by aluminium, some silicon and manganese would not be oxidised internally and hence some enrichment of these elements on the surface will occur during the annealing at a low dew point. Therefore better coating occurs at higher dew point.

Weldability

Weldability studies were carried out with samples heat treated in salt bath furnaces. Literature review[30-31] and a number of trials suggested that introduction of a post welding heating cycle could improve the weldability in terms of nugget diameter. Accordingly, a post welding heating was introduced in the final trial. The welded samples were subjected to tensile load in Instron 8801 with a cross head speed of 1mm/minute. The test results revealed significant improvement in terms of nugget formation and geometry, failure mode (exhibiting achievement of expected plug type mode of failure) and load of weld at failure [35].

No major disparity was apparent for the three different grades for the weld zone and the HAZ. However, superior properties were observed for grade 1 and grade 2 to that of grade 3.

4. Assessment of Structure Property Correlation Under High Strain Rate Testing

For high strain rate testing, another set of samples, cold rolled samples, cut in to required size (Fig. 2), for all three grades were heat treated as per above cycles in two adjacent salt bath furnaces for intercritical annealing and isothermal bainitic transformation (allowing shortest possible manual-shifting time from IA to IBT bath) followed by oil quenching to the room temperature. For high strain rate testing, the surfaces of the heat treated samples were made free from loose scales by grinding of emery papers and cleaned with acetone.

4.1. Characterisation

All tests for the high strain rate work were accomplished on a servo hydraulic Zwick/ Roell Re1 1852 high-speed tensile testing [located at IEHK, RWTH University, Aachen] machine including a digital measuring and controlling unit. The V_{max} and F_{max} for the machine are 10 m/s and 12 kN (to be reconfirmed) respectively. The tests had been carried out at strain rates 1 and 100 s^{-1} (average). Each test had been done for three times for Grade 1 and 2, and twice for Grade 3 due to paucity of material. German specification for dynamic tensile test [36], was followed for this work. The test pieces were made in accordance with the dimensions specified in

The strain rate was determined based on the available condition of the equipment. However, published experimental data and internal circulations of leading steel manufacturers [37] are in agreement with the maximum strain rate (100 s^{-1}) of the range selected here, to have resemblance with the crashing condition of passenger car components. For quasistatic test with a strain rate of $3.33 \times$

10^{-4} s^{-1} , data has been captured from Table 3.

The force measurement during the test was done using a piezoelectric load cell instrumented with a Weg Zimmer (opto-elektronisch) extensometer. The storage of test data was done with a 4-channel transient recorder (sampling rate 1 MHz, 10 bit analogue/ digital converter) and later for further calculation on a personal computer. To evaluate the results, the recorded data were first converted into technical stress strain diagrams allowing the determination of the mechanical properties by use of special software developed by IEHK, Aachen. At high strain rates the force signal was superimposed by oscillation, caused by the inertia of the test equipment, making the direct determination of the characteristics values impossible. Therefore a cubic spline was utilized to approximate the unfiltered stress-strain signal, allowing the gathering of the strength properties. Earlier works showed good conformity of results obtained in this way, using the load cell instrumented with strain gauges plus spline approximation, compared to the results achieved using the strain gauges fixed directly on the specimen [38].

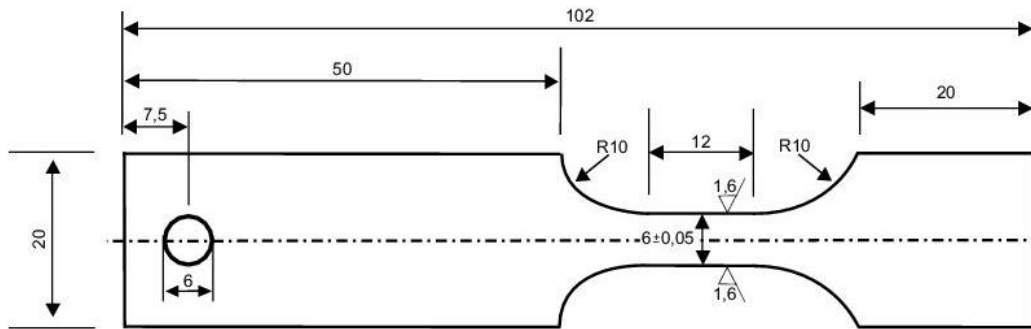


Figure 2. Specified sample geometry for high strain rate testing. All dimensions are in mm. The thickness of all the samples varied between 1.2 to 1.4 mm

4.2. Results and Discussion

The details of the test results for higher strain rate from dynamic tensile testing (1 and 100 s^{-1}) vis-à-vis the quasistatic properties are tabulated below (Table 5):

Table 5. High strain rate test results vis-à-vis quasistatic test results

Grade	Strain rate (s^{-1})	YS (MPa)	UTS (MPa)	YS/UTS	UTS/YS	Ag (%)	A_{Tot} (%)	n	Energy at 10% elongation (kJ/kg)	Energy _{Tot} (kJ/kg)	UTS x A MPa*%
1	QS	485	795	0.61	1.64	31	36	0.34	5.706	26.045	28,620
	1	493	764	0.65	1.55	24.3	35	0.298	8.689	32.017	26,740
	100	562	815	0.69	1.45	22.3	33	0.312	8.795	31.616	26,895
2	QS	511	849	0.60	1.66	23	29	0.27	6.313	21.087	24,621
	1	498	814	0.61	1.63	18.3	27.4	0.234	9.685	26.822	22,304
	100	580	858	0.68	1.48	18.5	28.4	0.255	9.352	28.485	24,367.
3	QS	521	959	0.54	1.84	19	23	0.26	6.989	18.955	22,057
	1	451	914	0.49	2.03	16.5	26.7	0.196	11.085	29.556	24,404
	100	539	971	0.56	1.80	15.2	27.8	0.21	10.62	31.089	26,994

(Grade 1: CMnSiAlP, Grade 2: CMnSiAlNb, Grade 3: CMnSiNb)
Energy_{Tot} : area under the stress strain curve

The yield strength for Grade 1 consistently increased from quasistatic to 100 s^{-1} whereas UTS initially decreased at 1 s^{-1}

and then increased at 100 s^{-1} crossing the quasistatic value (Fig. 3). But for grades 2 and 3, YS and UTS decreased at the intermediate level (i.e. at 1 s^{-1}) and then increased significantly at 100 s^{-1} , crossing the quasistatic value (Fig. 4 and 5).

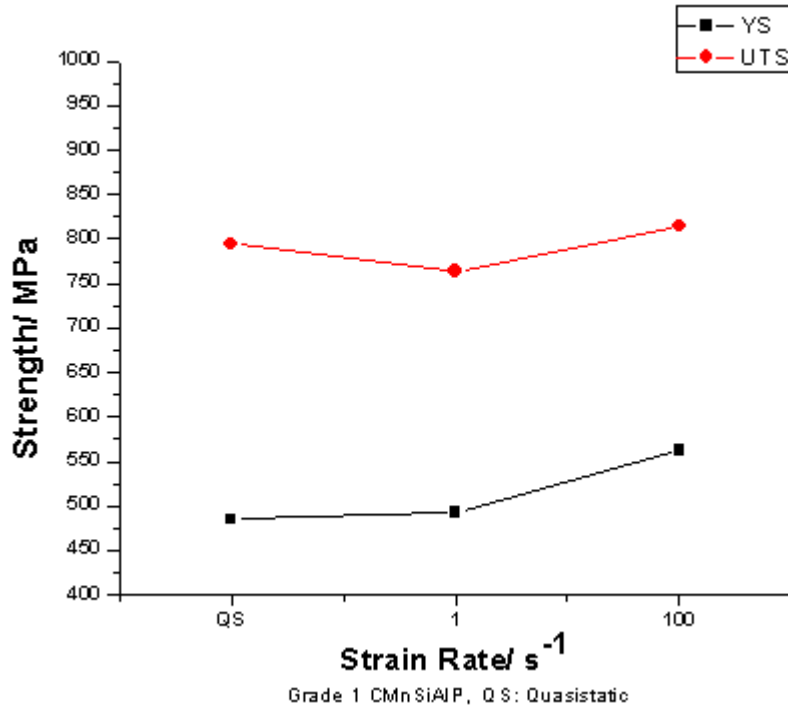


Figure 3. Variation of strength with respect to strain rate_ Grade1

Uniform elongation for all grades decreased from quasistatic through 100 s^{-1} (Fig. 6 to Fig. 7). Total elongation for Grade 1 decreased at 1 and 100 s^{-1} from the QS value consistently (Fig. 6). On the other hand, though it initially decreased at 1 s^{-1} , recovered at 100 s^{-1} and attained almost at the same level of the QS value for Grade 2 (Fig. 7). For Grade 3, the value increased from QS to 100 s^{-1} through 1 s^{-1} consistently (Fig.8).

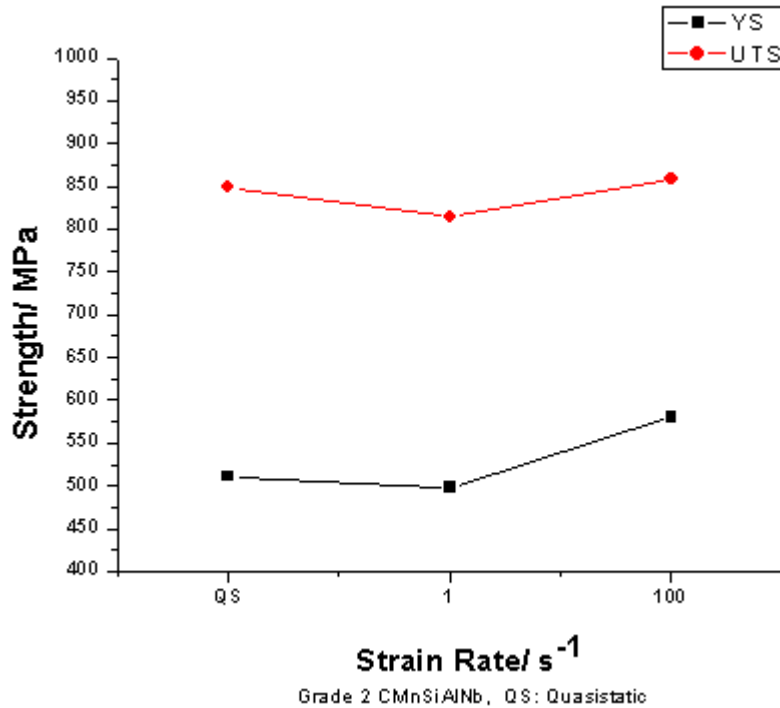


Figure 4. Variation of strength with respect to strain rate_ Grade2

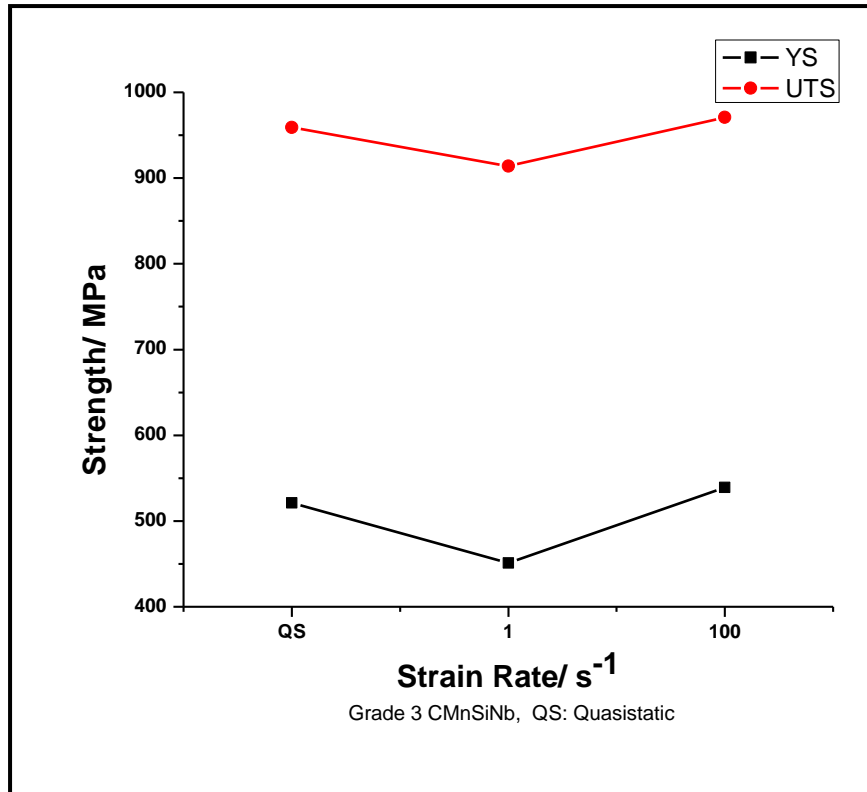


Figure 5. Variation of strength with respect to strain rate_ Grade3

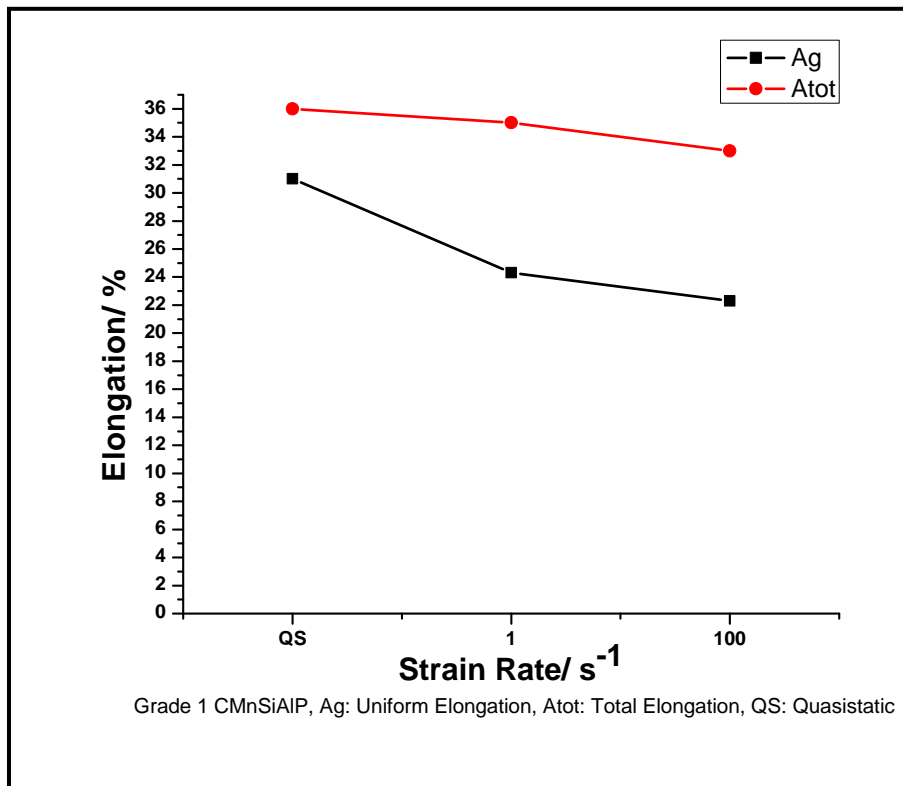


Figure 6. Variation of elongation (total and uniform) with respect to strain rate_ Grade1

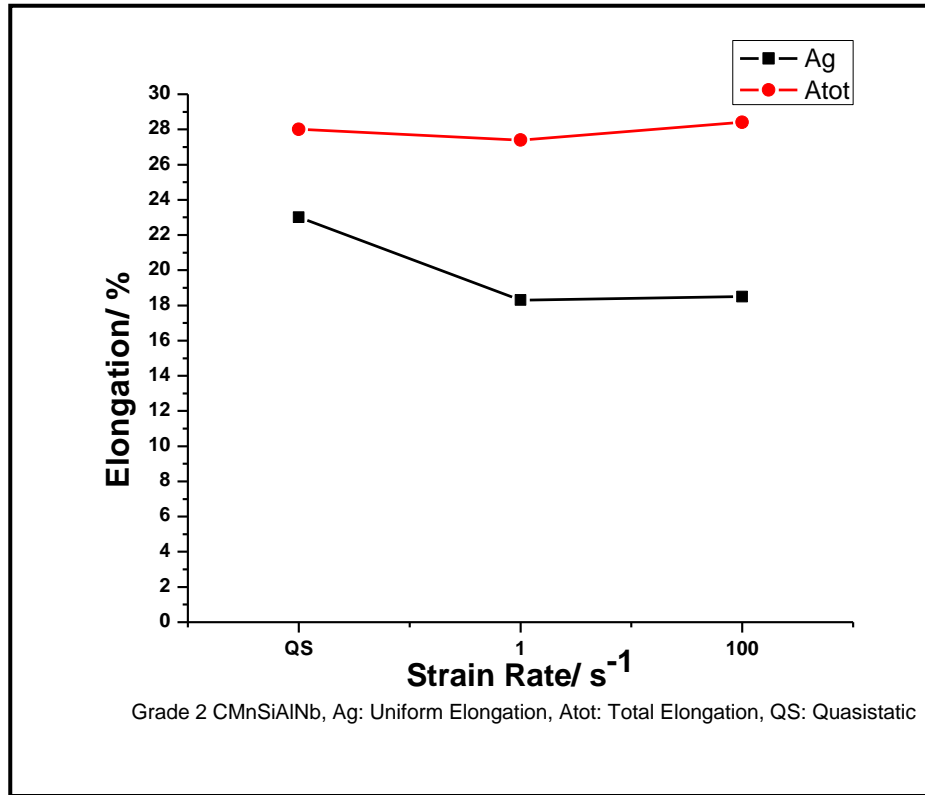


Figure 7. Variation of elongation (total and uniform) with respect to strain rate_ Grade2

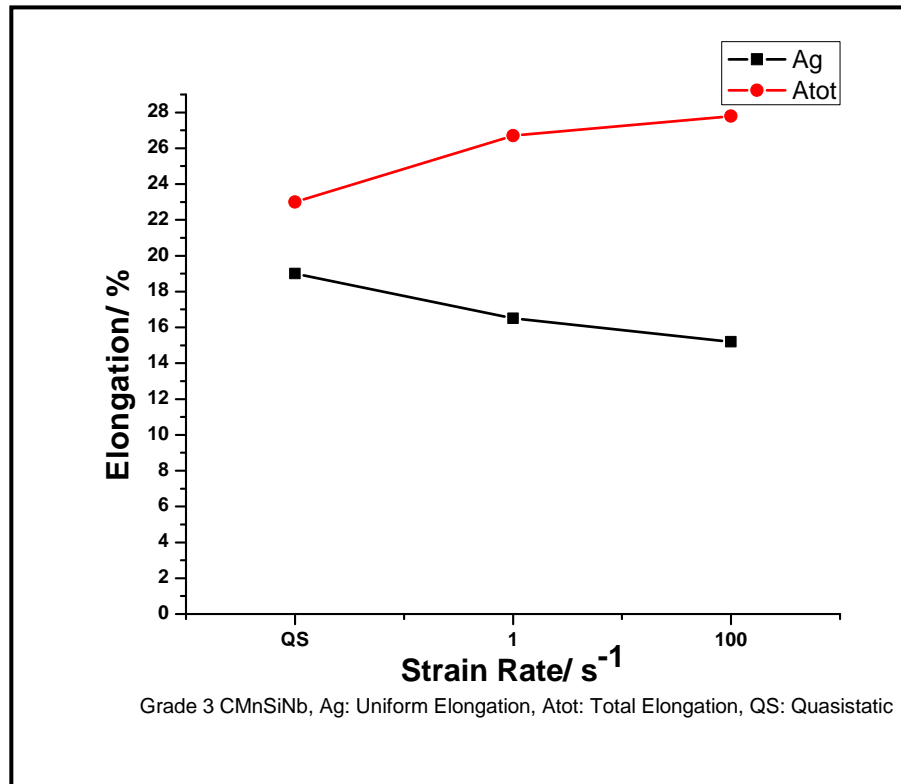


Figure 8. Variation of elongation (total and uniform) with respect to strain rate_ Grade3

Energy absorbed at high strain conditions reflects the ability to withstand crash conditions. Usually, energy absorbed during tensile test is expressed as the area under the

stress strain diagram, derived by integration. The multiplied value of the UTS and %total elongation is also considered as an indicator of the same.

This is also reported that the change of energy absorption with changing strain rate is predominantly guided by the elongation values. It is also estimated by several reported works that crash events involves a strain around 10% and the parts damaged in a crash will never be deformed until fracture. Therefore a rationale has been in place to compare the energy absorption of different steels by at a fixed elongation 10%. This is also envisaged that the adiabatic effect and the consequence of statistical scatter of extension is diminished[39].

For Grade 1, as observed in Fig. 9, the total energy (area under the engineering stress strain diagram) increases at strain rates 1 s^{-1} as well as 100 s^{-1} . Whereas, it has shown decrements at higher strain rates for UTS*% total elongation. Energy at 10% elongation increase from quasistatic to 1 s^{-1} and 100 s^{-1} and it is more or less unaltered for 1 s^{-1} and 100 s^{-1} strain rate.

For two other grades, same trend has been observed for energy at 10% elongation. The values were found in ascending order from Grade 1 to Grade 3 (Table 5 and Fig.9 to Fig. 11). For Grade2, the total energy is in continuous ascending order at 1 s^{-1} and

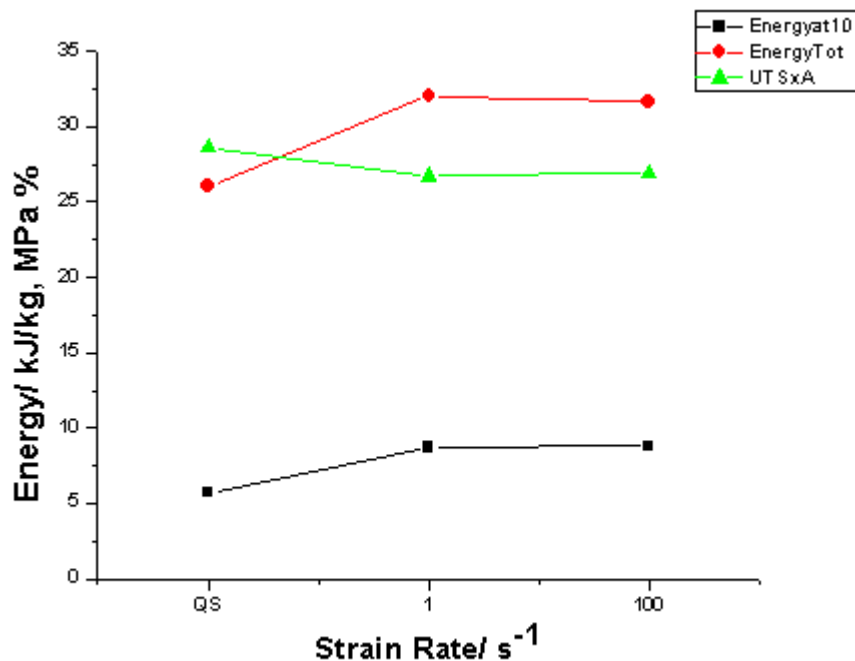
100 s^{-1} though UTS*% total elongation decreased at 1 s^{-1} and then crossed the QS value marginally (Fig. 10). For Grade 3, for total energy as well as UTS*% total elongation, noteworthy ascent has been observed (Fig. 11) as the initial energy at QS is lower than two other grades. This

phenomenon has been collated in comparative manner in Fig. 11.

Initial n-value at QS is highest for Grade 1 and lowest for Grade 3. At strain rate 1 s^{-1} , n-value decreased for all three grades and then it increased at 100 s^{-1} though it was lower than the initial (i.e. QS) values.

In general, it is evident from the assessment that reasonably high energy absorption for all strain rates is accomplished by TRIP steel. The absorption (UTS x Total Elongation) drops to a lower level during dynamic testing at the intermediate strain rate (here 1 s^{-1}) with an increase when strain rate rises (100 s^{-1}) except the Grade3 where an altogether steep rise has been observed. However, this development has likeliness with the trend of variation of strength and elongation.

For Grade 1 and Grade 2, the ratio of UTS and YS decreased continuously and on the contrary, the ratio of YS and UTS increased. Whereas for Grade 3 the ratio of UTS and YS increased at 1 s^{-1} and then decreased. Just opposite trend has been observed for the YS and UTS ratio. High UTS and YS ratio extends assurance for significant energy absorption and dissipation occurs during inelastic deformation. It also helps to avoid premature failure due to strain concentrations. Better material flow during forming is resulted from this also. However at high strain rate, it is lowered to some extent which has direct relation with the lower uniform elongation and n-value.



Grade1, QS: Quasistatic, Energyat10: at 10%, EnergyTot_Total Energy, UTSxA: UTSx% El

Figure 9. Variation of energy with respect to strain rate_Grade1

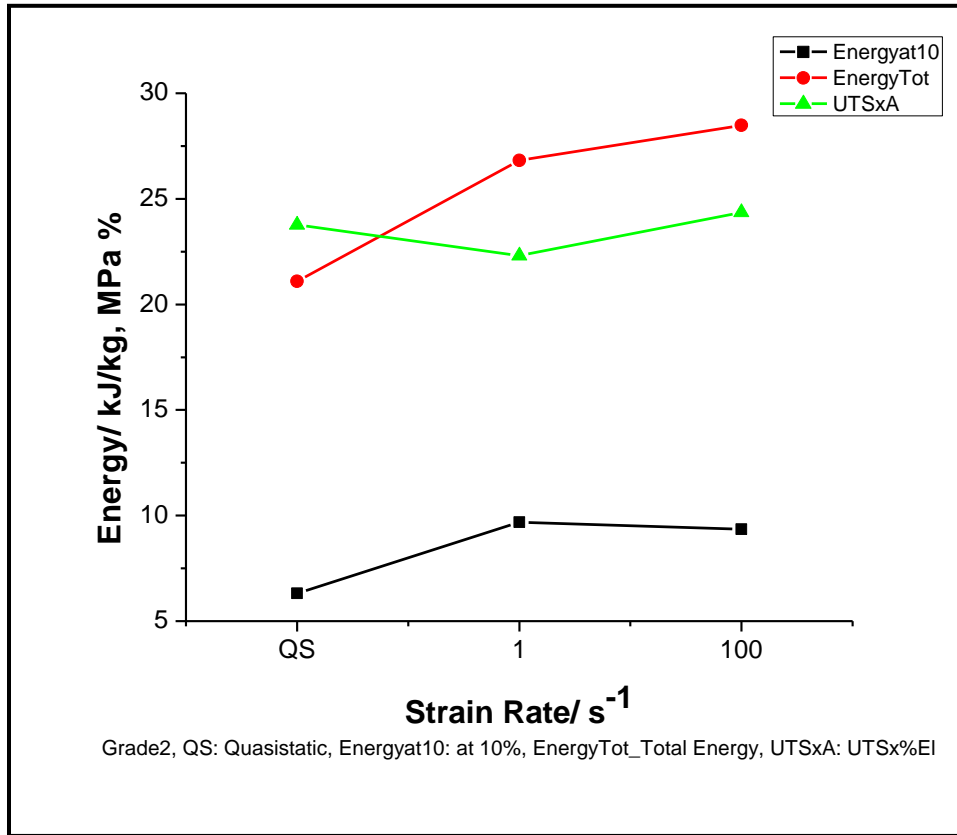


Figure 10. Variation of energy with respect to strain rate_ Grade2

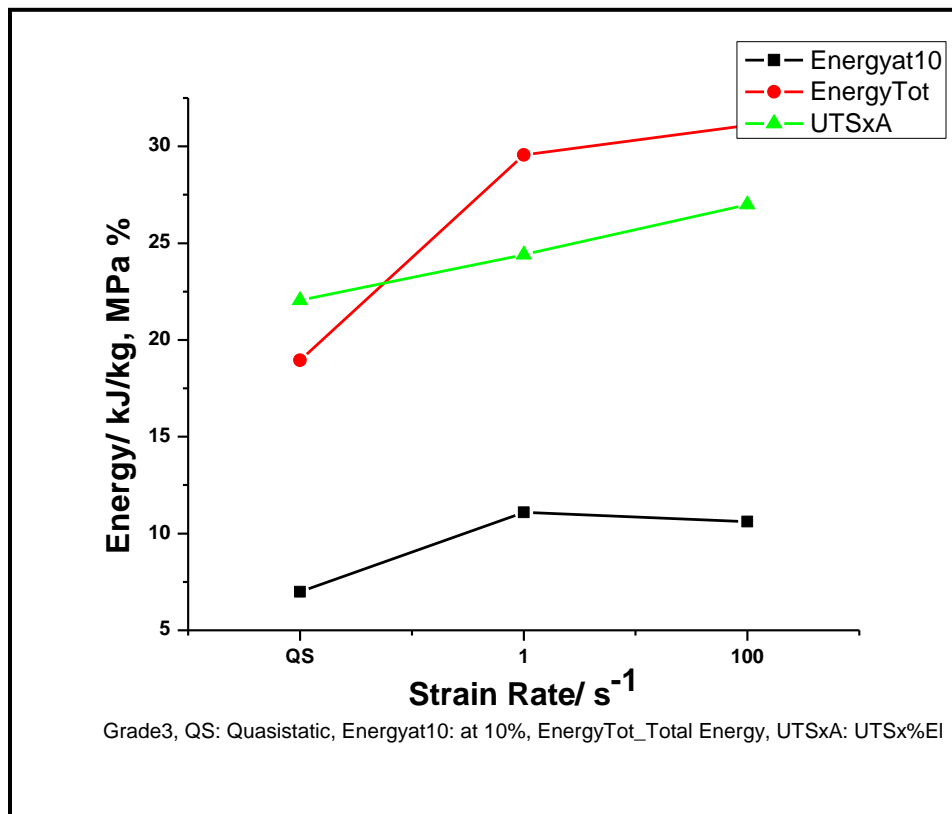


Figure 11. Variation of energy with respect to strain rate_ Grade3

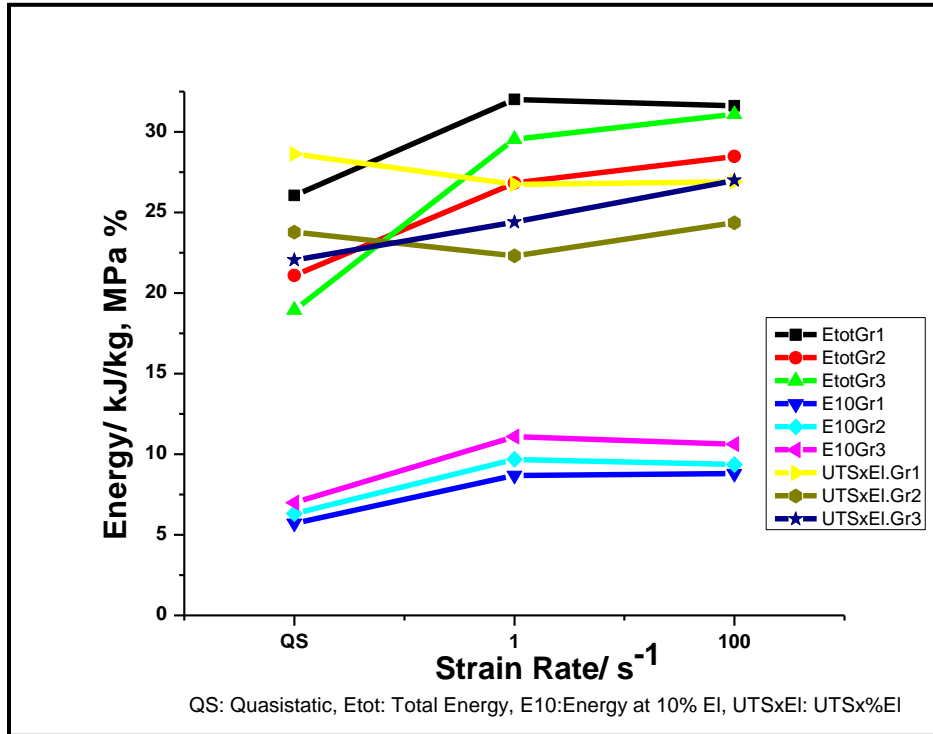


Figure 12. Comparative diagram on energy variation with respect to strain rate

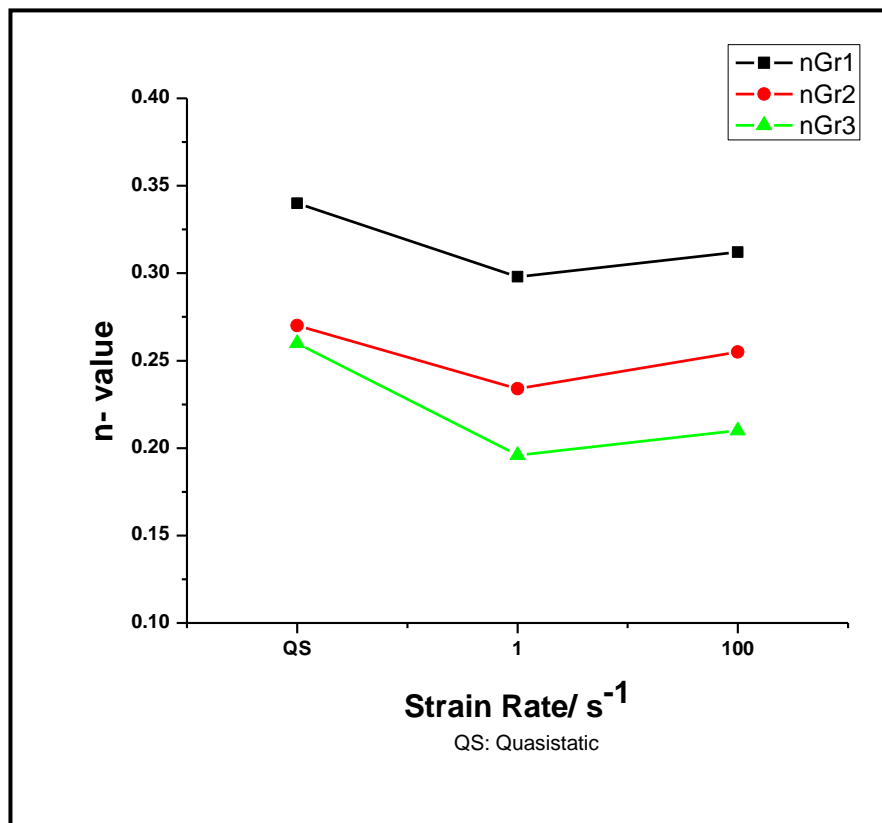


Figure 13. Comparative diagram on variation of n-value with respect to strain rate

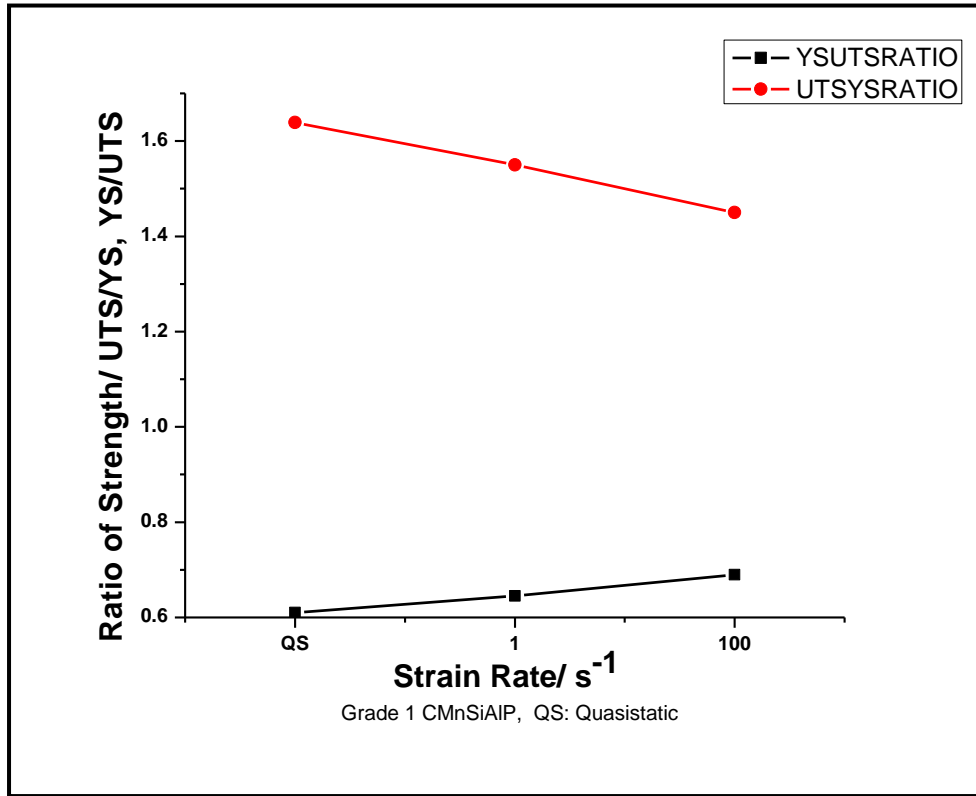


Figure 14. Variation of strength ratio with respect to strain rate_ Grade1

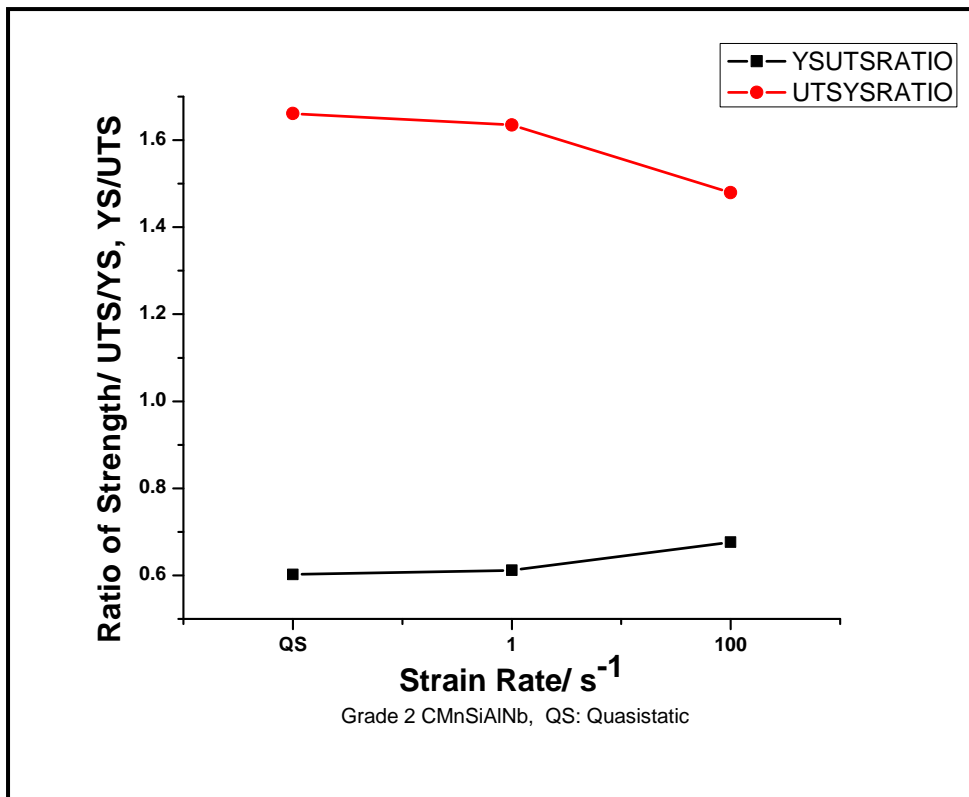


Figure 15. Variation of strength ratio with respect to strain rate_ Grade2

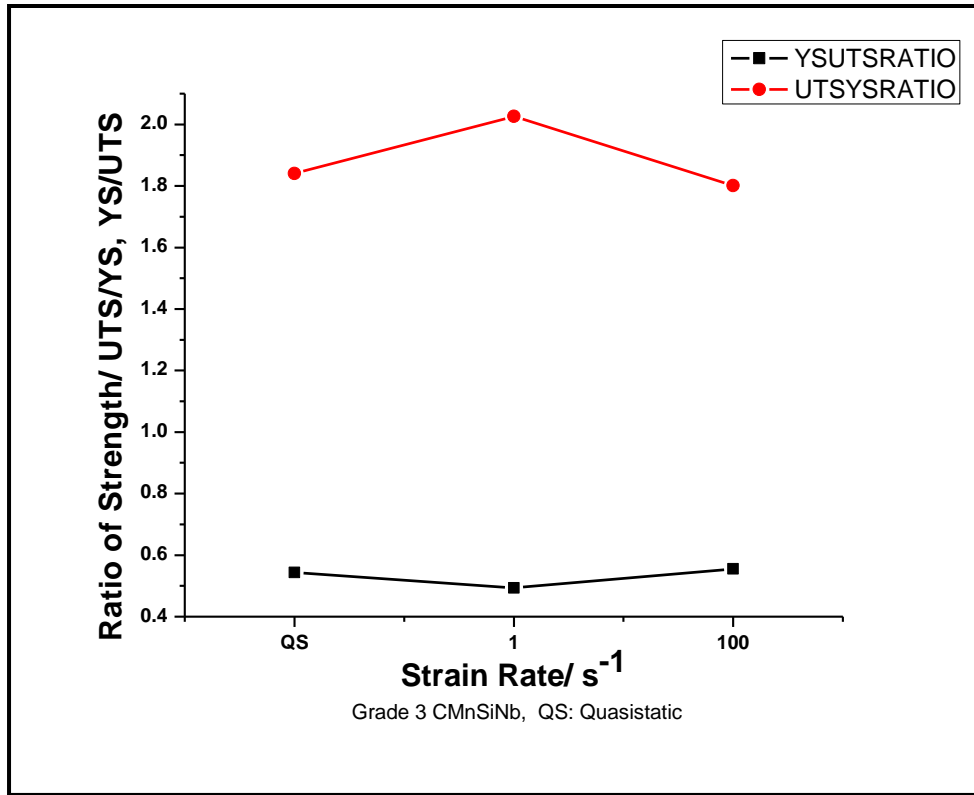
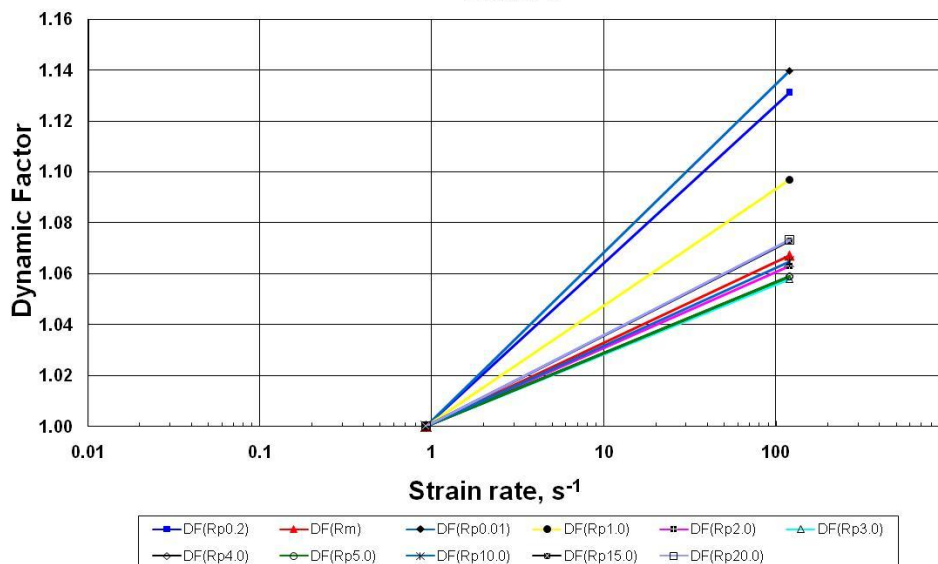
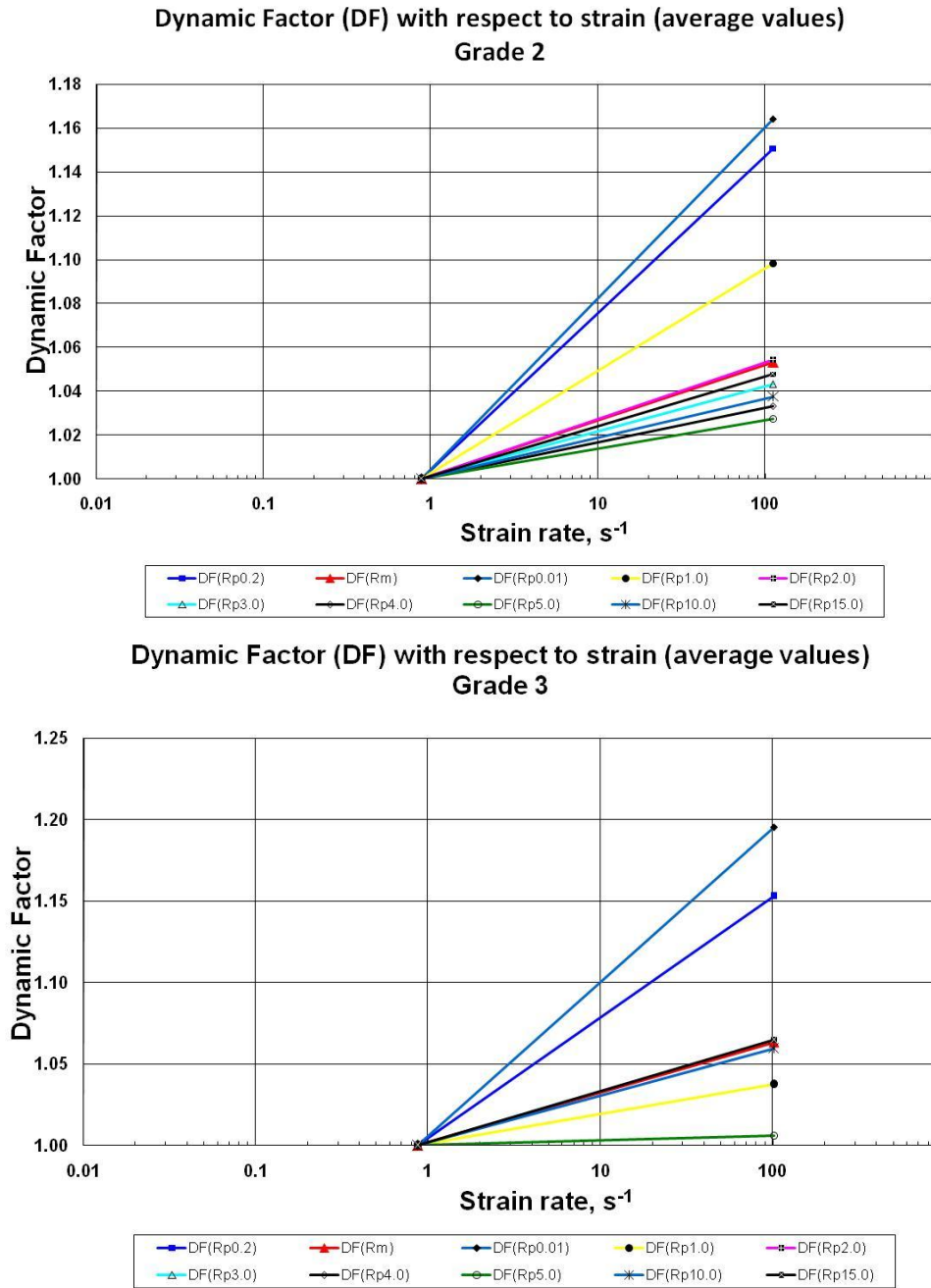


Figure 16. Variation of strength ratio with respect to strain rate_ Grade3

The basic difference between the high strain rate test and the quasi-static test is that inertia and wave propagation effects are more distinct at higher strain rates. These dynamic affects on test results at higher strain rates. When the strain rate is increased through the medium strain rate regime, the measurement of load is the first to be affected by stress wave propagation. The ratio between the strength at the higher strain rate (here 100 s⁻¹) against the lower strain rate (here 1 s⁻¹) at different strains are described as dynamic factor. This factor has got its highest value at yield point (Fig. 17). Again this dynamic factor is highest in Grade 3 CMnSiNb and lowest in Grade 1 CMnSiA IP. It might have a direct correlation with the maximum change of tensile strength vis-à-vis the energy absorption in Grade 3.

Dynamic Factor (DF) with respect to strain (average values)
Grade 1





Yield plateau is remarkably higher for dynamic tensile test (high strain rate testing) as observed in Fig. 18 to Fig. 20. This is maximum in 100 s^{-1} . During high speed deformation, it is envisaged that a huge accumulation of dislocations around hard phase for a very short time raises obstacle towards diffusion of dislocation as well as strengthening of ferrite substrate. The pronounced yield phenomenon is resultant of this effect.

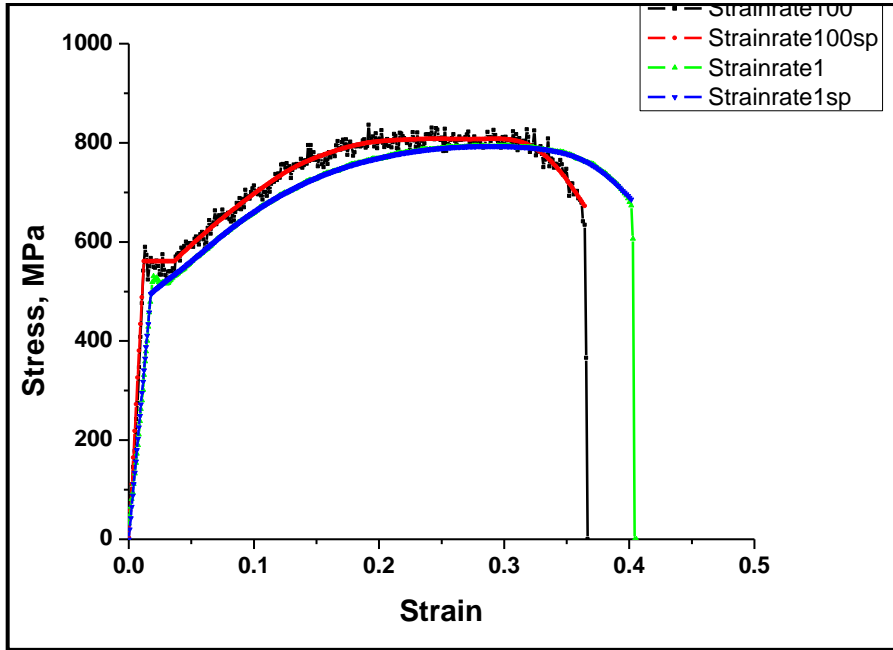


Figure 18. Engineering stress strain diagram for strain rates 1 and 100 s⁻¹ with and without spline (sp) for Grade 1_Specimen 1

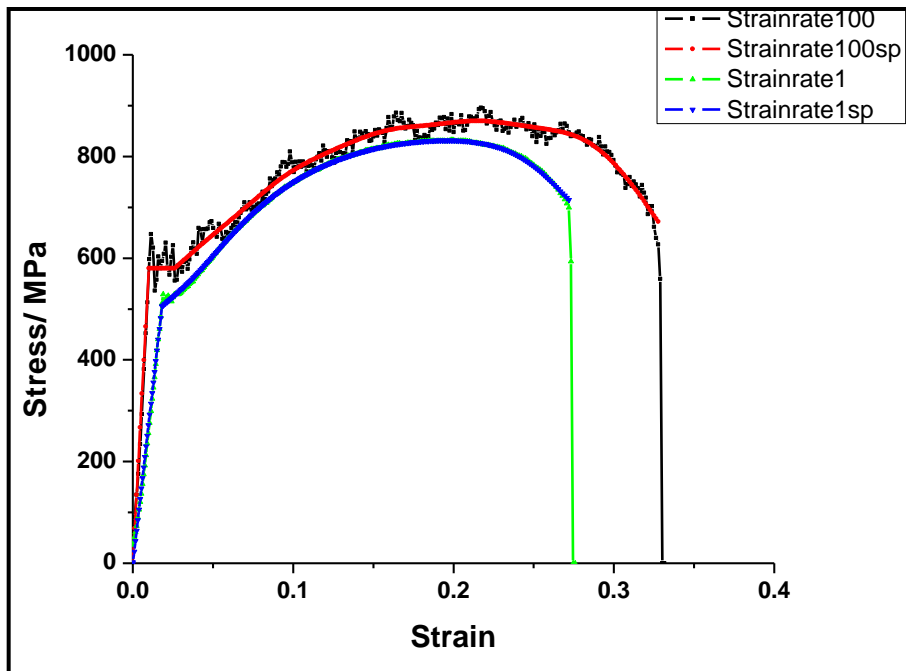


Figure 19. Engineering stress strain diagram for strain rates 1 and 100 s⁻¹ with and without spline (sp) for Grade 2_Specimen 1

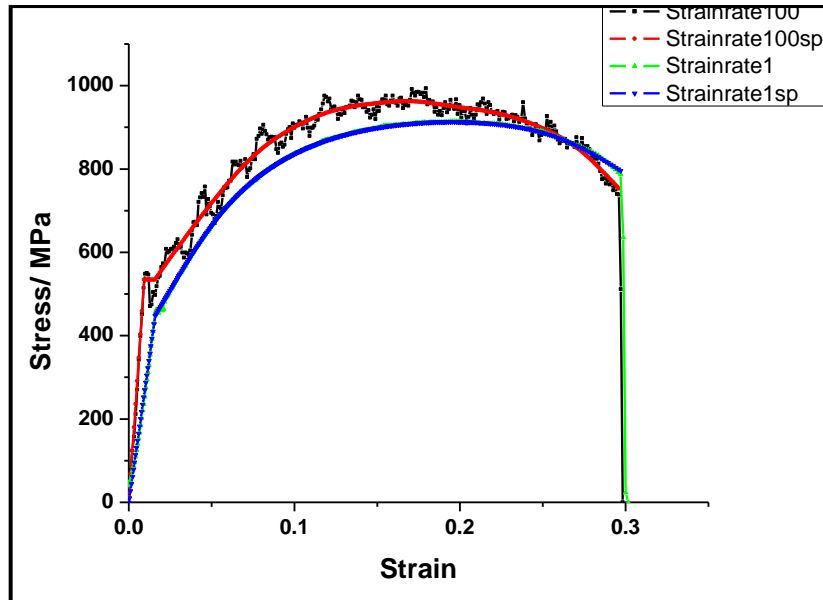


Figure 20. Engineering stress strain diagram for strain rates 1 and 100 s^{-1} with and without spline (sp) for Grade 3_Specimen 1

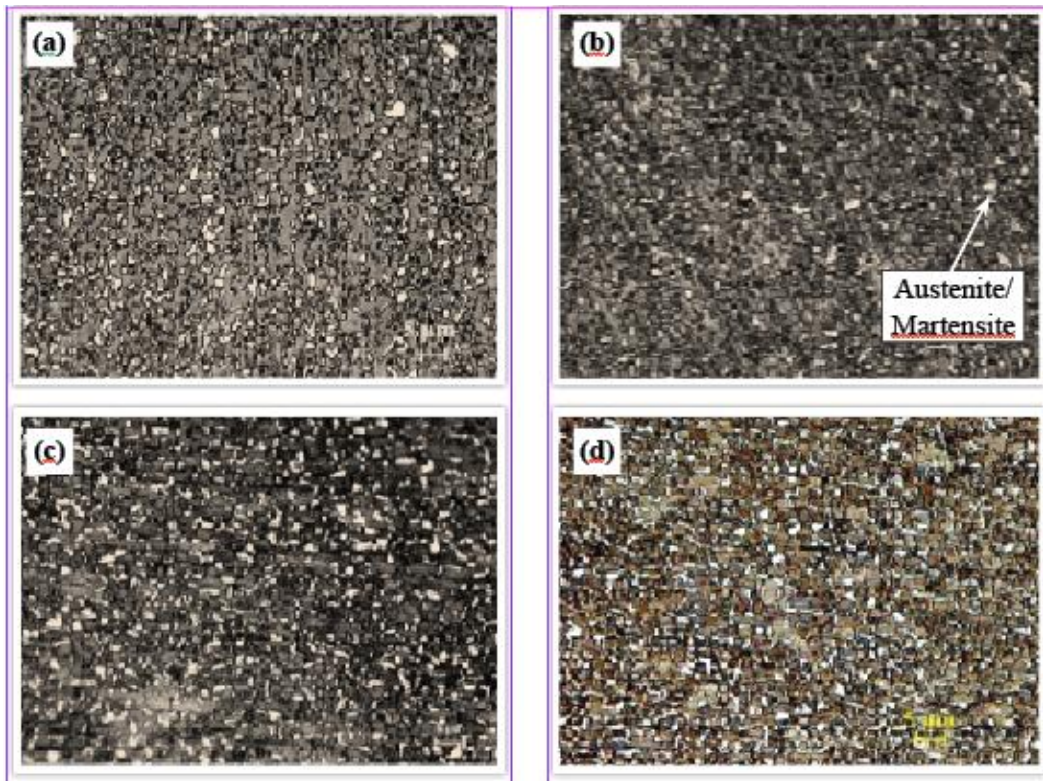


Figure 21. a to d show microstructure for Grade 2 after tensile test at 100 s^{-1} From fracture face towards the grip. Microstructure: Ferrite + Bainite + Austenite/Martensite (white phase)

Table 6. % Retained austenite in microstructure for Grade 2 after tensile test at 100 s^{-1}

Distance from fracture face (mm)	Fig.	% Retained austenite from XRD
3	21 a	NT
5	21 b	4
8	21 c	11
11	21 d	14

NT : not traceable properly

Microstructure of a representative sample showed presence of retained austenite even after high strain rate testing (Fig. 21a to 21 d, Table 6]. This carries the signature of transformation behaviour of austenite to martensite during deformation which is having a direct correlation with the TRIP property.

5. Conclusions

Three low carbon TRIP-aided steels have been developed through cold rolling, two step heat treatment and galvanising route. The material under study has shown very good performance under quasistatic as well as high strain rate tensile test resulting in high ultimate tensile strength with high total and uniform elongation. The material also has a high strain hardening exponent which has direct correlation with the availability of retained austenite in the microstructure after heat treatment.

The volume fraction of retained austenite measured through optical metallography had a reasonably good match with the value obtained through XRD technique. These values corroborated the amount of retained austenite predicted through artificial neural network model.

Changing the dew points, the coatibility have been improved and it has been observed that the samples with lower silicon and treated at higher dew point showed better coatibility during hot dip galvanising coating.

Trials for resistance spot welding have revealed that the steels are weldable. Introduction of post weld tempering cycles improves the weld nugget geometry, breaking load and failure mode under tensile shear loading

It is observed from the results that in general at high strain rates, the uniform elongation had shown decrement, whereas the total elongation and energy absorption were increased (except some deviations). The observations has corroborated various other works[30].

It is envisaged that during the high strain rate testing, temperature increases sharply which remains within the system. So this deformation mechanism is an adiabatic one which may play a significant role in restricting the extent of transformation of austenite to martensite[31], and thus, the reason behind the decrease in tensile strength during this adiabatic deformation can be explained due to the decrease of flow level and less transformation to martensite. The decrease in strength due to adiabatic deformation could also be due to the decrease in the flow level in accordance with the temperature dependence of yield point as well as due to decrease in strength decreases as exhibited in the temperature dependence of the strengthening graph[40].

For 1 s^{-1} , the impact of adiabatic heating being high, a trend of decrease in strength is very common. Whereas, for 100 s^{-1} , as the testing time is extremely low, that might not have much impact over the transformation of austenite to martensite resulted in higher martensitic transformation except Grade 3. Microstructure of Grade 3 has revealed that it had relatively lower austenite and there could have been

higher martensite as it had been evident from calculation of Ms temperature with the help of x-ray diffraction as well as calculation through Thermo-Calc.

Energy absorption is a function of tensile strength[41]. The tensile strength having been linearly proportional to the volume fraction of martensite in the structure[42, 43], presence of martensite from higher transformation of austenite or due to preexisting higher martensite, the energy level becomes higher. This has been reflected for higher energy levels for Grade 2 at 100 s^{-1} , and for Grade 3, both at 1 and 100 s^{-1} .

It is also established from this work that the behaviour at higher strain rate of the three developed steels, especially in terms of energy, have made them qualified to be applied to manufacture crash resistant components over the conventional high strength steels[44].

ACKNOWLEDGEMENTS

Authors are personally indebted to Prof. Wolfgang Bleck, Head, Department of Ferrous Metallurgy, IEHK, RWTH Aachen University for their support to carry out the work. Authors thankfully acknowledge Dr P K Banerjee, Chief (Actg.), R&D and Scientific Services, Tata Steel Ltd., Prof. S. Das, Head, Department of Metallurgical and Materials Engineering, IIT, Kharagpur, Authors are thankful to the Department of Science and Technology and Ministry of Steel, Government of India, International Bureau of the Federal Ministry of Education and Research, Germany for their partial financial support for the work. Authors also thank Prof. Subhabrata Datta of School of Materials Science and Engineering, Bengal Engineering and Science University, Shibpur, Howrah, Dipl. Ing. Christoph Keul, RWTH Aachen University, Dr. Monideepa Mukherjee of Tata Steel Ltd. for their hearty support.

REFERENCES

- [1] B. C. De Cooman, Current Opinion in Solid State and Material Science 8 (2004) 285-303.
- [2] V.F. Zackay, E.R. Parker, D. Fahr and R. Busch, Transactions of the American Society for Metals 60 (1967) 252-259.
- [3] B. Mintz and J.C. Wright, J.Iron and Steel Institute 208 (1970) 401-405.
- [4] E.M. Bellhouse and J.R. McDermid, Metallurgical and Materials Transaction A, Volume 41A (June 2010) 1460-1473.
- [5] P. Jacques, Q. Furne mont, A. Mertens, and F. Delannay: Philos. Mag. A, Vol. 81 (2001) 1789-1812.
- [6] J. H. Jung et al., 2008 International Conference on New Development in Advanced High Strength Steels, 25-37.

- [7] T. Heller and A. Nuss, Proceedings of the International Symposium on Transformation and Deformation Mechanisms in Advanced High Strength Steels, eds. M. Militzer, W. J. Poole and E. Essadiqi, CIM, Montreal (2003) 7-20.
- [8] O. Matsumura, Y. Sakuma and H. Takechi, Transactions ISIJ 21 (1987) 570-579.
- [9] W. S. Owen, Transactions of the American Society for Metals, 46 (1954) 812-829.
- [10] E. Girault, P. Jacques, Ph. Harlet, K. Mols, J. Van Humbeeck, A. Aernoudt, and F. Delannay, Materials Characterization 40 (1998) 111-118.
- [11] B. Mintz, International Materials Review 46 (2001) 169-197.
- [12] ASM Handbook, Vol. 6, Welding, Brazing and Soldering, ISBN 0-87170-383-3 (Dec. 1993) 405-407.
- [13] J. Maki, J. Mahieu, B. C. De Cooman, and S. Claesseur, Materials Science and Technology, Vol. 19 (Jan. 2003) 125-131.
- [14] W. Bleck, A. Frehn, and J. Ohlert, Proceedings of the International Symposium on Niobium, Orlando (2001) 727-752.
- [15] J. Gao and M. Ichikawa, Proceedings of the International Conference on Advanced High Strength Sheet Steels for Automotive Applications, AIST, Winter Park, Colorado (2004) 107-116
- [16] Chen et al., SE AISI Q (April 1991) 44-49.
- [17] D. Krizan, B. C. De Cooman and J. Antonissen, Proceedings of the International Conference on Advanced High Strength Sheet Steels for Automotive Applications, AIST, Winter Park, Colorado (2004) 205-216.
- [18] K. Hulka, W. Bleck and K. Papamantellos, Proceedings of the 41st Mechanical Working and Steel Processing Conference, Iron and Steel Society, Baltimore (1999) 67-88
- [19] X. Liu, P. Karjalainen, and J. Pertula, Thermo-mechanical Processing in Theory, Modelling and Practice" ed. W. Hutchinson et al., (1996), Stockholm, Sweden, 240-248
- [20] M. Onink, Th. M. Hoogendoorn and J. Colijn, Material Science Forum, 284-286 (1998), 185-192.
- [21] Debanshu Bhattacharya, Proceedings of the International Conference on Microalloyed Steels: Emerging Technologies and Applications (2007), Ed. Debashish Bhattacharjee et al., 50-60.
- [22] H. K. D. H. Bhadeshia and R. W. K. Honeycombe, Steels Microstructure and Properties, Third Edition, 2006, Elsevier Ltd.
- [23] Liesbeth BARBÉ, Kim VERBEKEN and Emiel WETTINCK, ISIJ International, Vol. 46 (2006), No. 8, 1251-1257.
- [24] J. Mahieu, S. Claessens, B.C. De Cooman, Metallurgical and Materials Transaction A Volume 32A, November 2001, 2905-2908.
- [25] ASM Handbook, Vol. 6, Welding, Brazing and Soldering, ISBN 0-87170-383-3 (Dec. 1993) 405-407
- [26] T. Herai et al, Resistance spot welding of high strength steel sheets, IIW Doc. III, 664-80
- [27] M. I. Khan, M. L. Kuntz, E. Biro and Y. Zhou, Materials Transactions, Vol. 49, No. 7 (2008) pp. 1629-1637.
- [28] Cretteur Laurent et al., Steel Research, ISSN 0177-4832, 2002, vol. 73, pp 314-319.
- [29] Yun Peng et al., Materials Science Forum Vols. 638-642 (2010) pp 3591-3596.
- [30] Rong TIAN, Lin LI, BC De Cooman, Xi-chen WEI and Peng SUN, Journal of Iron and Steel Research, International, Volume 13, Issue 3, May 2006, Pages 51-56.
- [31] Wolfgang Bleck and Ingo Sacheal, Steel Research 71(2000) No. 5—32.
- [32] Tanmay Bhattacharyya, Shiv Brat Singh, Sourav Das, Arunansu Haldar, Debashish Bhattacharjee, Materials Science and Engineering A 528 (2011) 2394–2400.
- [33] Tanmay Bhattacharyya, Shiv Brat Singh, Swati Sikdar Dey, Sandip Bhattacharyya, Wolfgang Bleck, Debashish Bhattacharjee, Materials Science and Engineering A, MSEA D12 02974 (under publication).
- [34] Indian Patent Application No. 633/KOL/10 of 11 .06. 2010.
- [35] Indian Patent Application No.1356/KOL/2011 of 21. 10. 2011.
- [36] Standard for high strain rate test, "Stahl Eisen Prüfblatt SEP 1230".
- [37] Internal Document, Corus
- [38] D. Stark-Seken, W. Bleck, W. Dahl, Materialprüfung, 37 (1995) 165-168.
- [39] I. D. Choi, D. M. Bruce, S. J. Kim, C. G. Lee, S. H. Park, D. K. Matlock, J. G. Speer, ISIJ International, 42 (2002) 1483-1489.
- [40] W. Bleck, Text Book on Material Testing for RWTH Students, Aachen University.
- [41] R.G. Davies, Metall. Trans. A, 10 (1979) 1549–1555.
- [42] R.G. Davies, Metall. Trans. A, 9 (1978) 671-679.
- [43] J. F. Butler, J. H. Bucher, Seminar on Vanadium Cold Passing and Dual Phase Steel, 18-20, Oct. 1978, Berlin.
- [44] R. G. Davies, C. L. Magee, Proc. Symp. On Structure and Properties of Dual Phase Steel, February 19-21, 1979, New Orleans, The Metal. Soc. AIME.